CIRRELT

CIRRELT-2023-02

Energy Efficient UAV-Based Last-mile Delivery: A Tactical-Operational Model with Shared Depots and Non-linear Energy Consumption Model

Maria Elena Bruni
Sara Khodaparasti
Guido Perboli

January 2023

Bureau de Montréal
Université de Montréal
C.P. 6128, succ. Centre-Ville
Montréal (Québec) H3C 3J7
Tél : 1-514-343-7575
Télécopie : 1-514-343-7121

Bureau de Québec
Université Laval,
2325, rue de la Terrasse
Pavillon Palasis-Prince, local 2415
Québec (Québec) G1V 0A6
Tél : 1-418-656-2073
Télécopie : 1-418-656-2624

Energy Efficient UAV-Based Last-mile Delivery: A Tactical-Operational Model with Shared Depots and Non-linear Energy Consumption Model

Maria Elena Bruni[1,*], Sara Khodaparasti[2], Guido Perboli[2,3]

[1] Department of Mechanical, Energy and Management Engineering, University of Calabria, Italy

[2] Department of Management and Production Engineering, Polytechnic University of Turin

[3] Interuniversity Research Centre on Enterprise Networks, Logistics and Transportation (CIRRELT)

Abstract. This paper studies the drone-aided last-mile delivery problem with shared depot resources. Our research motivation comes from E-commerce logistics, where big companies such as Amazon, are already filing up patents for the development of drone-friendly fulfillment centers towers that could serve as both charging hubs and convenient pit stops for delivery drones to pick up and drop off packages efficiently. We mainly focus on the tactical decisions about the selection of shared fulfillment centers used as the drone launch and retrieve stations and the fleet size plans. The operational drone route decisions are also incorporated into a unified framework to account for the mutual impact between tactical and operational plans. Moreover, we consider explicitly the non-linear and load-dependent nature of the energy consumption function for drone batteries. The problem is formulated as a mixed integer program with linear constraints, developed in the realm of layered networks, where the non-linear nature of energy consumption and its load dependency are incorporated and efficiently handled without the need of approximating non-linear terms.

Keywords: Last-mile delivery, E-commerce, Drone delivery, UAV, non-linear energy consumption, multi-depot routing problem.

---

* Corresponding author: mariaelena.bruni@unical.it.

Dépôt légal – Bibliothèque et Archives nationales du Québec
Bibliothèque et Archives Canada, 2023

1 Introduction

The two digits growth of the e-commerce is reshaping the distribution of goods in our cities and the associated logistic business processes and models. Its disruptive impact on the delivery process has dramatically challenged transportation companies [19, 21], not only for the increased volume of last-mile deliveries, but also for the consequent change in customers, more connected and informed, and whose orders are smaller, more frequent and normally characterized by very tight time-windows (up to 1 hour). This pushes the companies to explore new delivery methods, such as cargo bikes, lockers, delivery robots [6, 20]. Among these options, one of the more interesting one, both from an industrial and an academic point of view, are Unmanned Aerial Vehicles (UAVs), also known as drones.

Drone-aided deliveries offer significant benefits in terms of cost and delivery time savings [1, 3, 18] together with lower CO2 emissions and congestion [5], especially compared to terrestrial vehicles. In addition, drones often represent the unique option to get access to distant and/or isolated areas, for their ability to travel across different directions and altitudes. Acknowledging such potentials, Amazon released a number of patents for multi-level Fulfillment Centers (FC)s that facilitate drone landing and take-off within the delivery operations, especially in populated urban settings [2], but other similar systems are under test, as Google's "Project Wing" [13], DHL's "Parcelcopter" [8], and the joint venture between Swiss Worldcargo (the air freight division of Swiss International Air Lines) and the California-based start-up Matternet [7].

Generally speaking, FCs are, in fact, drone stations that are centrally controlled and are built in a beehive-like tower shape to ease the accommodation of a large number of drones. The FCs also provide retail companies with a variety of different services from package handling to recharge operations. The use of such facilities, in a shared way can be an opportunity for retail companies interested in drone delivery services.

Although the idea of shared FCs seems so appealing, there are some tactical challenges to cope with. In practice, the agreement between the retailer and the FCs owner is a long-term contract to specify the set of shared FCs selected by the retailer and the required amount of space at each center for stocking the parcels. This also depends on the fleet size, which is another important decision the retailer should take in advance. Since tactical and operational decisions are highly connected and influenced by each other,

addressing the tactical decisions without considering the impact of operational plans may lead to system failure and severe losses. To account for such mutual effect, the tactical and operational plans should be addressed simultaneously in a unified framework. Moreover, drone battery consumption plays a key role in the planning and optimization of drone operations. Unfortunately, this component is highly non-linear, with a consequent increase in the complexity of the problem at hand.

To cope with these issues, the main contributions of this paper are the following.

- We present an integrated model to jointly address both tactical and operational decisions arising in the drone-aided delivery context.
- Differently from the majority of the literature, we integrate the non-linear drone battery energy consumption. In particular, Dorling et al. [9] showed that drone energy consumption is a non-linear function of drones' payload and travel time. Clearly, considering the highly non-linear nature of the energy consumption function enhances the realism of the models, but exacerbates their complexity.
- We formulate the drone routing problem with non-linear and load-dependent energy consumption as a Mixed Integer Linear Problem (MILP).
- We conduct an extensive set of computational experiments, using data that reflect the main issues involved in the problem.

The rest of the paper is organized as follows. In Section 2, we review the relevant contributions to the drone-aided routing problem. In Section 3, we describe the problem, provide a brief discussion on drone battery energy consumption, and present the MILP. In Section 4, we comment on the computational experiments. Finally, Section 5 summarizes the paper and presents directions for future research.

2 Literature review

In this Section, we briefly cover the literature on the pure-play drone-based models which focus on drone usage to deliver parcels directly from depots to customer sites. In order to place our contribution in the right perspective,

among the pure drone routing problem contributions, we also address those involving depot/drone base/station/fulfillment center location/selection decisions.

The acknowledgment of the importance of appropriate energy consumption models in the literature on the pure-drone routing problem led to the formulation of energy consumption as an explicit function of drone payload and travel time. The work of Dorling et al. [9] is one of the first studies that recognized the non-linear nature of the energy consumption in drone batteries. The main assumptions made are that the power consumed during takeoff, or landing is approximately equivalent to the power consumed while hovering and the thrust balances the weight force. To avoid the computational intractability of non-linear constraints, the energy consumption function is replaced by its linear approximation. The authors proposed two multi-trip drone routing formulations with different objective functions (either total operating cost or total delivery time) and designed a simulated annealing heuristic to solve the model. Similarly, Cheng et al. [4] applied a linear approximation of the load-dependent energy consumption function in a multi-trip drone routing problem. The model is enriched by valid cuts embedded into a branch-and-cut algorithm. In [24], the drone maximum payload, maximum flight duration and customers' time windows are considered in a multi-trip routing context. The energy consumption is approximated as a linear function of drone weight and travel time. Rabta et al. [22] studied a drone routing problem for parcel delivery with the possibility of en-route charge from a single depot, considering the energy consumption linearly dependent on the distance and the payload. The model is tested on a small example with 1 depot, 1 recharging station and 5 customers.

In a recent paper, Du et al. [10] proposed a MILP formulation for the drone routing problem with the aim of minimizing the total customer service time and drone flight time. The model considered constraints on drone payload, maximum flight distance, and customer time windows. The authors applied a Dantzig–Wolfe decomposition approach to solve an instance of the problem for medical supply delivery.

Regarding the scientific literature in the location-routing field, some authors adopted a hierarchical approach in which first the location decisions are tackled separately and next the operational drone-routing plans are addressed; others addressed the strategic/tactical location plans and operational routing decisions simultaneously. Clearly, the suitability of each approach depends on the application context; for instance, in a server-centric

application, where the strategic location decisions are irreversible and costly, especially compared to the operational routing decisions, it makes sense to adopt a hierarchical framework; on the contrary, in a customer-centric context, where the delivery plans are highly affected by the location of drone bases, it is more reasonable to simultaneously handle both location and routing decisions.

Table 1 categorizes the recent scientific literature. Specifically, we classify the contributions based on *Depot selection/location decisions* (whether addressed hierarchically or simultaneously), *Fleet sizing* decisions, critical energy consumption-related features such as *drone payload*, *flight distance/duration* and *Energy consumption constraints*.

Table 1: Summary of multi-depot drone routing problems

	Depot selection decision	Fleet sizing	Drone payload	Flight distance/ duration	Explicit energy consumption constraints
Torabbeigi et al. [23]	H	✓	✓	✗	Linear
Kim et al. [15]	H	✓	✓	✓	✗
Liu et al. [17]	S	✓	✗	✓	✗
Yakıcı [25]	S	✓	✗	✓	✗
Kim et al. [14]	S	✓	✓	✓	✗
Li et al. [16]	S	✓	✗	✓	✗
Grogan et al. [12]	S	✓	✗	✓	✗
This paper	S	✓	✓	✗	Non-linear

H: Hierarchical S: Simultaneous.

Concerning the first stream (hierarchical approach), Torabbeigi et al. [23] proposed two mathematical formulations involving strategic and operational plans to optimize the drone routes for parcel delivery. At the strategic level, a set covering model determines the minimum number of required depots to cover all customers, next, at the operational stage, a drone routing model is solved to find the optimal drone routes minimizing the number of dispatched drones. The authors included energy consumption constraints into the problem which are linear functions of the payload and the travel time. A variable pre-processing algorithm and primal and dual bound generation methods are developed to speed up the computational performance. Kim et al. [15] proposed a set covering model to find the optimal locations of drone depots, followed by a multi-depot drone pickup and delivery model, in a healthcare context. The cost of used drones is minimized while the drone payload and the maximum drone flight time constraints are satisfied. A pre-processing algorithm, a partition method, and a Lagrangian relaxation methods are

developed as solution approaches.

In the location-routing context, Liu et al. [17] presented a model in a drone patrol application to simultaneously find the optimal location of drone launching bases and the optimal drone routes minimizing the total cost (base establishment cost, drone usage cost, and flight cost). The authors imposed a maximum flight duration for drones. Two heuristic algorithms combined with local search strategies are designed and tested for 25 target points and 5 potential base stations. Yakıcı [25] proposed a selective location-routing problem with the aim of maximizing the sum of importance values corresponding to the covered points. The model accounts for a maximum flight time and considers an upper bound for the number of selected stations to be used. An ant colony optimization metaheuristic is designed as solution approach. Kim et al. [14] proposed a drone routing model with multiple depots, and multiple drones, allowing multiple UAVs to deliver goods to one customer at the same time. The objective function minimizes the delivery and drone usage costs. The drone payload capacity and maximum flight distance are considered as constraints. The optimal location of selected depots, the fleet size, and the drone routes are the output of the problem. The model is solved for instances up to 75 customers. In another paper, Li et al. [16] studied a multi-depot drone routing problem to minimize the total number of drones used and the total traveled distance. The model accounts for a maximum drone flight time. Since not all the depots are required to be used, the optimal location of used depots is an output of the problem. To solve the problem, the authors developed a heuristic approach based on a hybrid large neighborhood search.

In a recent paper, Grogan et al. [12] addressed a drone application for relief operations conducted after a tornado. The authors proposed a routing problem considering the maximum drone endurance limit with the aim of minimizing the maximum route duration. The number of dispatched drones and occupied depots are the problem outputs.

To conclude, in order to address the energy consumption concept in drone-aided last-mile delivery, the majority of contributions only implicitly account for the limited battery capacity imposing some constraints on the maximum drone flight range. It is easy to note that, apart from the present contribution, only Torabbeigi et al. [23] explicitly accounted for the drone battery energy consumption. In this case, however, a strong simplification of the problem is made since battery consumption is expressed as a linear function of payload and travel time. Clearly, this assumption makes the problem more tractable

but it raises questions about the feasibility of designed routes, as we will show in the computational results. The contribution is also different from the present paper since the authors dealt with the depot location plans and routing decisions separately.

In this paper, we aim to fill this gap since we explicitly account for the non-linear nature of energy consumption while tackling the tactical depot selection/fleet size and operational routing decisions simultaneously. Clearly, this exacerbates the computational intractability of the problem but enables the decision-maker to adopt tactical policies which enhance operational efficiency.

3 Problem description and mathematical formulation

In this Section, we introduce the Drone Routing Problem with Shared Depots (DRP-SD) and provide a brief discussion on the non-linear load-dependent drone energy consumption. Next, we formulate the problem as an efficient MILP, developed based on a load-indexed layered graph [11].

3.1 Problem definition

The DRP-SD is a location routing problem that determines the optimal subset of shared FCs used as drone launch and retrieve stations, the optimal size of the fleet to be deployed, and the optimal drone routes. The choice of the FCs to use is guided by the minimization of the total cost: the tactical cost related to the FC tariffs (for packaging and handling services), the fleet usage cost, and the operational delivery cost. The retailer can afford to rent a limited number of FCs and each FC can host up to a pre-specified number of drones.

A fleet of homogeneous drones is available to deliver homogeneous parcels. The drone batteries are fully charged at the beginning of the service. The drone routing decisions define the FC that launches the drone, the order of customers to be visited, and the FC that retrieves the drone, that can be different from the starting FC. Once the route plans are defined, the drone is appropriately loaded and visits the subset of customers assigned. Clearly, the designed routes should be *energy feasible*, i.e. the total energy consumed should not exceed the battery capacity. Since the drone energy

consumption depends on travel time and (non-linearly) on the drone payload, it is important to track, at each customer's site, the drone payload after dropping the parcel at the customer's doorstep. Finally, after delivering the last customer's package, the drone is retrieved at one of the FCs.

It is important to note that in the DRP-SD, the main focus is on tactical plans such as the selection of FCs and the fleet size decision, while the operational routing plans are incorporated to account for the connection and mutual interactions between such long-term and short-term plans. As mentioned earlier, at the time the tactical decisions are planned, the exact information on the parcels features such as weight is not available and we plan based on peak- or average-demand scenario, depending on the risk aversion of the decision maker.

Figure 1 represents a DRP-SD instance with four potential FCs and three drones. In the colored squares above each customer, the accumulated drone payload after departure from the customer is reported. All parcels have a weight of 0.5 kg. Each drone is launched from a selected FC, serves multiple customers and is finally retrieved at one of the active FCs already used as drone launch points. As we can see, the choice of FCs is selective and one FC is not used.

3.2 DRP-SD: Mathematical formulation

Following Dorling et al. [9]'s approach, the energy consumption (in Watt-hours, Wh) in a drone flying from point i to point j with travel time t_{ij} while carrying a payload of weight p_{ij} can be expressed as:

$$E_{ij} = \sqrt{\frac{g^3}{2\,\rho\xi h}}\,(\omega + \mu + p_{ij})^{3/2}\,t_{ij} \tag{1}$$

where g represents the gravity constant (in N/kg), ρ denotes the fluid density of air (in kg/m^3), ξ is the area of spinning blade disc (in m^2), h is the number of drone rotors [4] and ω and μ represent, respectively, the drone frame and battery mass (in kg). Clearly, modeling the energy constraints with non-linear payload-dependent energy function as in (1) entails the definition of non-linear constraints. Thanks to the problem assumption on the demand homogeneity and to the use of load-indexed layered graphs, it is possible to embed the non-linear energy consumption in a MILP.

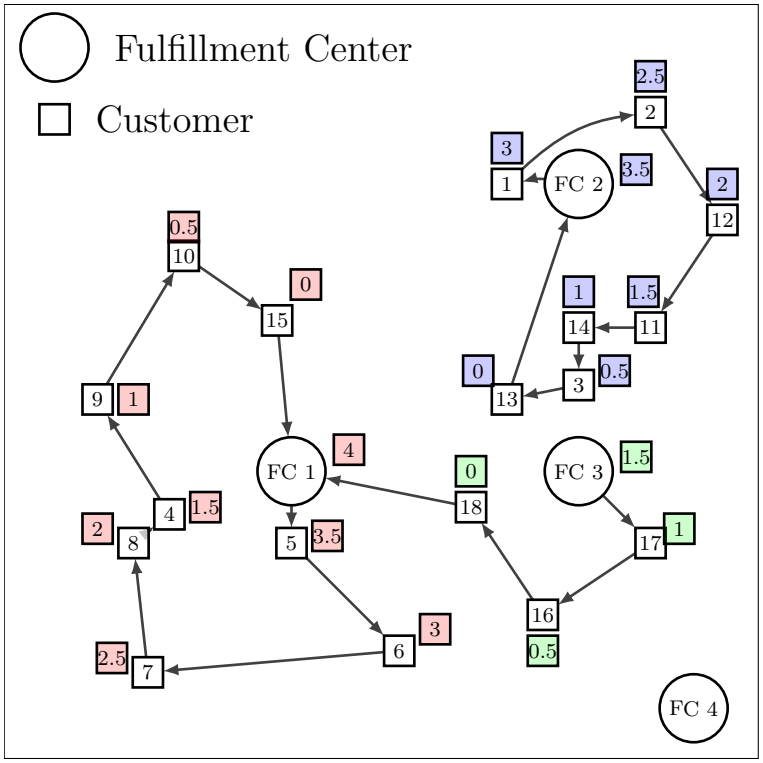

Figure 1: DRP-SD solution

The load-indexed layered graph is built upon indexed levels, which correspond to different drone payloads. To be more specific, let p be the parcel weight of each customer and Q be the maximum payload capacity of the drone. Clearly, the drone can serve up to $N = \lfloor \frac{Q}{p} \rfloor$ customers. Now, if the parcels have weight U, $(U \leq Q)$, the drone payload after delivering the order of the $r-$th customer is $(U - r\,p)$ that corresponds to the load-index/level of $(U - r\,p)$. When the drone is on its trip back to the FC, its carrying payload is 0, which corresponds to the load index of 0. We may represent the load-indexed layered graph as displayed in Figure 2. This graph includes different load levels from N to 0 where each load index represents the drone carrying payload just after visiting a customer. Any node in the graph represents either one of the customers (denoted by squares and indexed from 1 to n), or one of the FCs (displayed by circles and indexed from 0, 1, ..., m) and the level assigned to the node represents the drone payload (the number of packages to be delivered) upon arrival at the node and before serving it. The

auxiliary node 0 is used to connect the starting FC to the first customer. The last customer is followed by the FC that retrieves the drone. Figure 3 displays the load-indexed layered graph corresponding to the example in Figure 1. Notice that thanks to the layered graph, the energy consumption associated to each load level r can be easily evaluated as

$$\epsilon_r = \sqrt{\frac{g^3}{2\,\rho\xi h}}(\omega + \mu + r\,p)^{3/2}$$

and hence, becomes a parameter. Defining load indexed decision variables, as reported in Table 2 (where the whole notation is reported), the DRP-SD can be formulated as the following MILP:

Sets and indices	
$C = \{1, \cdots, n\}$	Set of customers, indexed by i, j
$D = \{1, \cdots, m\}$	Set of potential FCs, indexed by d
$D' = \{0\}$	Auxiliary node
$L = \{0, 1, \cdots, N\}$	Set of levels, indexed by r
Parameters	
c_{ij}	Travel cost between (i, j)
ν_d	Weight-based tariff of the FC d
p	Customer's package weight
δ	Drone usage cost
FS	Fleet size
Cap_d	Capacity of the FC d
T	Maximum number of FCs to use
ϵ_r	Constant parameter $\sqrt{\frac{g^3}{2\rho\xi h}}(\omega + \mu + r\,p)^{3/2}$
E	Battery capacity
Decision variables	
x_i^r	Binary variable which takes value 1 if customer i is visited at load-level r (upon arrival at the location of customer i, the drone carries r parcel packages)
y_{ij}^r	Binary variable which takes value 1 if node j is visited right after node i and there are exactly $r-1$ parcels to be delivered after
z_d	Binary variable which takes value 1 if FC d is used
ϵ_i	Continuous variable that indicates the accumulated energy consumption upon arrival at node i

Table 2: Mathematical model: notation

$$\min: \sum_{i\in C}\sum_{\substack{j\in C\\ j\neq i}}\sum_{r\in L} c_{ij}\,y_{ij}^r + \sum_{d\in D}\sum_{j\in C}\sum_{r\in L}\nu_d\,p\,r\,y_{dj}^r$$

$$+\sum_{j\in C}\sum_{r\in L}\delta y_{0j}^r \tag{2}$$

$$\sum_{r\in L} x_i^r = 1 \quad i\in C \tag{3}$$

$$\sum_{r\in L}\sum_{j\in C} y_{0j}^r \leq FS \tag{4}$$

$$\sum_{i\in C} x_i^1 = \sum_{r\in L}\sum_{j\in C} y_{0j}^r \tag{5}$$

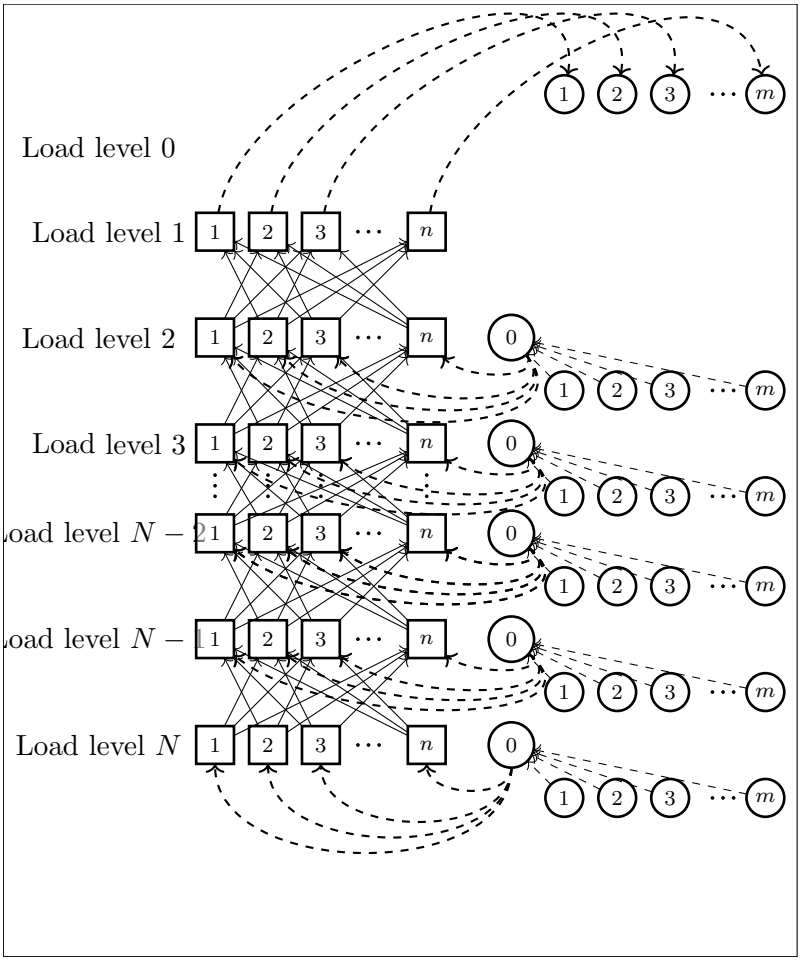

Figure 2: Load-indexed layered graph

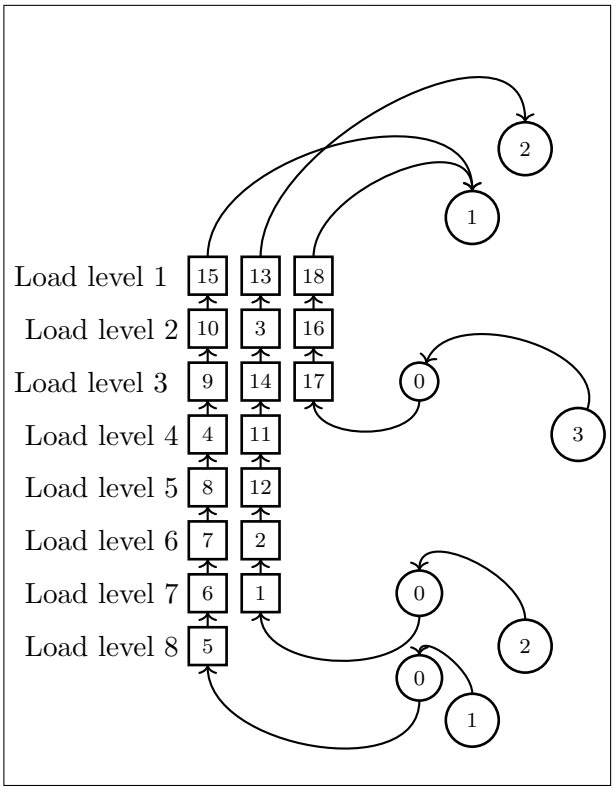

Figure 3: Load-indexed layered graph for example in Figure 1

$$x_j^1 = \sum_{i \in D} y_{ji}^0 \quad j \in C \tag{6}$$

$$\sum_{\substack{j \in C \\ j \neq i}} y_{ij}^r = x_i^{r+1} \quad i \in C,\, r \in L, r \neq N \tag{7}$$

$$\sum_{\substack{i \in C \cup \{0\} \\ i \neq j}} y_{ij}^r = x_j^r \quad j \in C,\, r \in L,\, r \neq N \tag{8}$$

$$y_{0j}^N = x_j^N \quad j \in C \tag{9}$$

$$\sum_{d \in D} y_{dj}^r = y_{0j}^r \quad j \in C,\, r \in L,\, r \neq 1 \tag{10}$$

$$\sum_{j \in C} y_{jd}^0 \leq \sum_{\substack{r \in L \\ r \neq 1}} \sum_{j \in C} y_{dj}^r \quad d \in D \tag{11}$$

$$\sum_{j \in C} \sum_{r \in L} y_{dj}^r \leq Cap_d \quad d \in D \tag{12}$$

$$z_d \geq y_{dj}^r \quad d \in D,\, j \in C,\, r \in L,\, r \neq 1 \tag{13}$$

$$\sum_{d \in D} z_d \leq T \tag{14}$$

$$e_d + \sum_{\substack{r \in L \\ r \neq 1}} \epsilon_r t_{dj} y_{0j}^r \leq e_j +$$

$$M'_{dj}(1 - \sum_{\substack{r \in L \\ r \neq 1}} y_{dj}^r) \quad d \in D,\, j \in C \tag{15}$$

$$e_i + \sum_{\substack{r \in L \\ r \neq N}} \epsilon_r t_{ij} y_{ij}^r \leq e_j +$$

$$M_{ij}(1 - \sum_{\substack{r \in L \\ r \neq N}} y_{ij}^r) \quad i,\, j \in C, i \neq j \tag{16}$$

$$e_j + \epsilon_0 \sum_{d \in D} t_{jd} y_{jd}^0 \leq E \quad j \in C,\, d \in D \tag{17}$$

$$x_i^r \in \{0, 1\} \quad i \in C,\, r \in L \tag{18}$$

$$y_{ij}^r \in \{0, 1\} \quad i,\, j \in D \cup C \cup D',\, i \neq j,\, r \in L \tag{19}$$

$$z_d \in \{0, 1\} \quad d \in D \tag{20}$$

$$e_i \geq 0 \quad i \in C \tag{21}$$
$$e_d = 0 \quad d \in D \tag{22}$$

The objective function (2) minimizes the total cost. Constraints (3) ensure that each customer is visited exactly once. Constraint (4) expresses the restriction on the maximum fleet size. Constraints (5) and (6) ensure that all the drones are retrieved back at the end of the service. Constraints (7)-(9) represent the connectivity constraints and express the relation between the binary variables x_i^r and y_{ij}^r. According to constraints (7), any customer i visited at the upper level $r+1$ should be connected to exactly one customer (let say j) at level r by traversing link $(i,\ j)$. Constraints (8) guarantee that each customer j visited at level r should be linked to exactly one customer (let say i) or connected directly to the auxiliary node 0 by the link $(0, j)$ in the same level. Constraints (9) require that customers visited at level N should be visited right after the auxiliary node 0 via arc $(0, j)$ in the same level. Constraints (10) define the relation between y_{0j}^r and y_{dj}^r variables. Constraints (11) ensure that only the FCs selected as drone launch sites can retrieve the drones back. Constraints (12) represent the restriction on the FCs' capacity. Constraints (13) allow drones dispatch only from selected FCs. Constraints (14) impose an upper bound on the number of selected FCs. Constraints (15)-(17) express the drone energy consumption: notice that, thanks to the load-indexed graph, the payload of the drone in each level r can be represented as constant rp, as embedded into the parameter ϵ_r. Constraints (15) is for the first visited customer, (16) for the remaining customers. M_{ij} and M'_{dj} are large enough constant that make the constraints binding only when the corresponding y variables take value one. Constraints (17) limit the total energy consumed to the battery capacity. Finally, constraints (18)-(21) express the nature of variables and constraints (22) set the initial accumulated energy consumption.

4 Computational results

In this Section, we report the computational results conducted on two sets of instances with 50 and 75 customers. The data set with 50 customers is taken from the benchmark [4]. In order to test the model on larger instances with 75 customers, we have extended the 50-customer instances by adding 25 new customers where the demand and the coordinate location of

the new customers were randomly generated from the range of demand and coordinate locations for the 50-customer instances. As in [4], the travel time between customers i and j is set equal to the travel distance between nodes i and j, calculated according to the Euclidean norm. The delivery cost is set as $c_{ij} = \alpha\, t_{ij}$ where $\alpha = 0.94\,\$/h$ is the delivery cost per hour. The drone usage cost δ was set to $0.7\,\$$ and the FC tariff is computed as $\nu_d = \frac{\delta}{\gamma}$ (the parameter $\gamma \in \{5, 10\}$ represents the proportion between the FC tariff and the drone usage cost). For all experiments, we have considered 5 potential FCs with a capacity of at most 5 drones ($Cap_d = 5$), and $T = 4$. Depending on the instance size, we have set $FS = 10$ or $FS = 12$.
Regarding the spatial configurations of the FCs, we have considered a *Centered* configuration, where the FCs are located close to the center of the delivery area, and a *Marginal* configuration, where the facilities are marginally located around the outskirt of the area. In more details, let (X_i, Y_i) be the location coordinates of customer i in the 2-dimensional space, we define

$$\begin{aligned} \bar{X} &= \frac{1}{n}\sum_{i\in C} X_i \\ \bar{Y} &= \frac{1}{n}\sum_{i\in C} Y_i \\ R_X &= X_{max} - X_{min} \\ R_Y &= Y_{max} - Y_{min} \end{aligned} \tag{23}$$

where $X_{min} = \min_{i\in C} X_i$, $X_{max} = \max_{i\in C} X_i, Y_{min} = \min_{i\in C} Y_i$, $Y_{max} = \max_{i\in C} Y_i$ For the centered configuration the coordinates of the five FCs are:

FC1 : $(\bar{X}, \bar{Y})$

FC2 :$(\bar{X}, \bar{Y} - \beta R_Y)$

FC3 : $(\bar{X}, \bar{Y} + \beta R_Y)$

FC4 :$(\bar{X} - \beta R_X, \bar{Y})$

FC5 : $(\bar{X} + \beta R_X, \bar{Y})$

where the input parameter $\beta \in (0, 1)$ controls the dispersion among the FCs for the centered configuration (we set $\beta = 0.2$ in all experiments). For the marginal configuration the coordinates of the FCs are:

FC1 : (X_{min}, Y_{min})

FC2 : (X_{max}, Y_{min})

FC3 : (X_{min}, Y_{max})

FC4 : (X_{max}, Y_{max})

FC5 : $(\frac{X_{min}+X_{max}}{2}, Y_{min})$

We have considered a MATRICE 600 PRO drone with a payload of $6\,kg$ and six TB47S batteries with a power of $0.099\,kWh$. The estimated parcels weight is $0.8\,kg$.
All the experiments have been performed on an Intel® Core i7-10750H, with 2.60 GHz CPU, 16 GB RAM working under Windows 10 and Gurobi 9.1 has been used as MILP solver.

4.1 Energy consumption versus flight range

In order to highlight the importance of dealing with energy consumption in the drone-delivery context, we have first carried out a set of experiments on the instance $50-5$ and marginal configurations of the FCs, with the following input parameters $T = 4$, $Cap_d = 2$, $FS = 6$, $\phi = 5$. For the considered drone, the flight time endurance is $\zeta = 16\,min$. This flight time has been evaluated considering the drone always flying fully loaded. This is a quite conservative assumption, since in practice, the drone is never in this situation. Despite this, in the results we will show that it may happen that the drones have not enough energy to complete the route.
We have compared three different models reflecting different modeling approaches for drone endurance: the *Energy-based Model*, *Flight Range Model* and the *No energy Model*.

The *Energy-based Model* incorporates (1) embedded into the MILP model, as discussed in Section 3; the *Flight Range Model* implicitly accounts for the limited battery consumption, limiting instead the total flight time for each drone. To be more precise, the energy-related variables e_i and their corresponding constraints are removed; instead, a set of continuous variables t_i, $i \in D \cup C$ are introduced denoting the flight duration upon arrival at node i. Also, constraints (24)-(27) are added into the model to set the flight duration upon arrival at a customer and to limit the flight duration.

$$t_i + \sum_{r \in L} t_{ij} y_{ij}^r = t_j \; i \in C \cup D, \; j \in C, i \neq j \tag{24}$$

$$t_j + \sum_{i \in D} t_{ji} y_{ji}^0 \leq \zeta \; i \in D, \; j \in C \tag{25}$$

$$t_i = 0 \; i \in D \tag{26}$$

$$t_i \geq 0 \; i \in C \tag{27}$$

The *No energy Model* is obtained by excluding the variables e_i and the corresponding set of constraints.

Table 3 reports the comparative results for the models discussed earlier. The energy consumption and flight duration are specified in columns with headings EC and FD, respectively.

As can be observed in Table 3, in both the *Flight Range Model* and *No energy Model* some drones violate the battery capacity which means the routing plans specified by an asterisk are neither valid nor reliable in practice. On the other hand, the *Energy-based Model* not only provides feasible routes, but it also gives more balanced solutions, where the drones are evenly used. In fact, the average flight duration (in minutes), for the *Flight Range Model* is 11.67 with a variation among drones of 7.38 minutes. The same values for the *No energy Model* are 11.43 and 6.54 minutes while for the *Energy-based Model*, we get 10.54 and 3.30 minutes. It is interesting to note that the *Energy-based Model* provides the best performance especially compared to the *Flight Range Model*. In fact, not only the *Flight Range Model* fails to provide energy-feasible routes, but it even provides larger flight times both in terms of the average value and the spread amongst different drones.

Table 3: Comparative results: energy consumption versus flight range

Energy-based Model		Flight Range Model		No energy Model	
EC (kWh)	FD (min)	EC (kWh)	FD (min)	EC (kWh)	FD (min)
0.085	10.38	0.052	8.16	0.052	8.16
0.077	9.54	0.089	11.46	0.077	9.54
0.091	12.06	0.095	11.40	0.095	11.40
0.078	9.24	0.085	10.44	0.085	10.44
0.075	8.76	0.111*	12.90	0.111*	12.90
0.085	11.16	0.093	10.80	0.118*	14.70
0.099	11.70	0.132*	15.54	0.107*	11.64
0.096	11.52	0.101*	12.72	0.101*	12.72

4.2 Model validation and discussion

Table 4 displays the results for instances with 50 customers where for each instance, we have considered 2 different γ values (5 and 10) and 2 FC configurations, for a total of 20 instances. The first three columns in Table 4 display the instance-related information.

In terms of computational time, all the instances are solved in less than 11 minutes and, on average, the CPU time is about 3 minutes. The columns FCC and VC represent, respectively, the percentage of the tactical *Fulfillment center Cost* and the *Vehicle Cost* over the total costs expressed as $FCC = \frac{\sum_{d\in D}\sum_{j\in C}\sum_{r\in L}\nu_d\, p\, r\, y^r_{dj}}{Obj}\,100$ and $VC = \frac{\sum_{j\in C}\sum_{r\in L}\delta y^r_{0j}}{Obj}\,100$. In a similar way, DC represents the percentage of the operational *Delivery Cost* over the total costs $DC = \frac{\sum_{i\in C}\sum_{j\in C}\sum_{r\in L} c_{ij}\, y^r_{ij}}{Obj}\,100$. We have also reported the average *Arrival Time* (Avg_{AT}) to the customers and the average *Energy Consumption* over all the drones (Avg_{EC}) as important *Key Performance Indicator*s (KPIs). Finally, the last column reports the number of drones (out of 8) that require at least 80% of a fully charged battery to complete the route.

The following observations can be drawn from the results. On average, FCC and VC are about 39% and 54% of the total cost, while DC is limited to 7%. Such results are expected since, in general, tactical costs are higher than operational costs. The average customer's waiting time is just about 3 minutes, showing a speedy delivery and implying good customer satisfaction. In addition, the average energy consumption is about 79% of a fully

charged battery. This is an informative insight since the fluctuations in energy consumption, mostly due to weather-related disruptions can drastically affect the validity of designed routes. In this case, an energy buffer of 20% contributes to the robustness of the routing plans. When $\gamma = 10$, the contribution of FCC and VC are, on average, 30.86% and 61.72% of the total costs incurred to the system showing that the VC is two times the FCC. Instead, in the case of $\gamma = 5$ (that corresponds to doubled FC tariffs), the average share of FCC and VC are equal to 47.14%. In terms of the delivery cost, no significant variation is observed (the average DC of 5.75% in case of $\gamma = 5$ compared to the average DC of 7.47% corresponding to $\gamma = 10$).
Second, regarding the KPIs, the average arrival time clearly is not affected by the increase in FC tariffs and the slight variation in the average energy consumption is related to the flexibility of the proposed model to choose any of the FCs as the drone retrieve sites as long as the battery capacity is respected.

Regarding the spatial configuration of FCs, we can draw two important insights. First, by switching from the centered to the marginal configuration and under the same tariff setting, the total system cost slightly increases due to the increase in the total traveling cost. Needless to say, marginal areas of the city are less populated while most of the customers are closer to the city center and farther from the marginal FCs. Clearly, when the tariffs are the same, it is more beneficial to utilize the FCs near the city center which ensures speedy delivery and lower energy usage.
The second insight comes from the comparison of the centered configuration with higher tariffs ($\gamma = 5$) and the marginal one with lower tariffs ($\gamma = 10$). In many real-world applications, the FCs located on the outskirts of the city incur in lower tariffs compared to those in the city center. Nonetheless, the marginal configuration can be quite appealing since the tactical costs can be reduced. If the marginal configuration is adopted, the drones should fly longer distances to reach the customers and this, in turn, will increase the operational delivery cost, and other time or distance-related KPIs.

For instance, under the marginal configuration, the tactical cost decreases by 50% but, instead, the delivery costs increase from 2% and up to 8%. In addition, the Avg_{AT} KPI, under the marginal case, is always worse than the centered one (at least 4% and at most 21.57% higher). Under the centered case at most half of the drones consume an amount of energy which is more than 80% of the drone capacity while under the marginal setting, this value may increase with an average energy consumption always above the

Table 4: Computational results: benchmark instances

Instance	γ	FC configuration	FCC (%)	VC (%)	DC (%)	Avg_{AT} (min)	Avg_{EC} (kWh)	$> 80\%$	Obj	CPU (s)
50-1	5	Centered	47.15	47.15	5.70	3.06	0.072	3	11.87	39.95
	10		30.84	61.69	7.45	3.06	0.075	3	9.07	44.37
50-2	5	Centered	47.13	47.13	5.72	3.30	0.076	3	11.88	53.36
	10		30.83	61.67	7.48	3.30	0.073	3	9.08	127.34
50-3	5	Centered	47.31	47.31	5.74	3.06	0.073	4	11.83	138.92
	10		30.98	61.97	7.52	3.06	0.072	4	9.03	84.14
50-4	5	Centered	47.22	47.22	5.54	3.12	0.076	4	11.85	102.17
	10		30.91	61.83	7.25	3.12	0.074	3	9.05	148.03
50-5	5	Centered	47.32	47.32	5.34	2.88	0.073	4	11.83	11.29
	10		30.99	61.99	7.00	2.88	0.072	2	9.03	14.82
50-1	5	Marginal	46.94	46.94	6.11	3.72	0.081	5	11.92	235.51
	10		30.67	61.34	7.98	3.72	0.084	6	9.12	463.87
50-2	5	Marginal	47.07	47.07	5.85	3.42	0.081	5	11.89	642.59
	10		30.78	61.56	7.65	3.42	0.088	7	9.09	380.15
50-3	5	Marginal	47.03	47.03	5.93	3.72	0.081	5	11.90	242.78
	10		30.74	61.49	7.76	3.72	0.082	6	9.10	398.82
50-4	5	Marginal	47.11	47.11	5.77	3.54	0.083	6	11.88	151.50
	10		30.81	61.63	7.55	3.54	0.084	6	9.08	268.39
50-5	5	Marginal	47.13	47.13	5.73	3.42	0.088	8	11.88	116.90
	10		30.83	61.66	7.49	3.42	0.078	5	9.08	43.21

$0.078\,kWh$ (this value is below $0.076\,kWh$ under the centered configuration).

Table 5 reports the results for the larger instances with 75 customers. The optimal fleet size is equal to 11 drones for all cases and the average CPU time is about 17 minutes; as expected, the solution time increases with the instance size. Regarding the FCC and VC, we observe that if $\gamma = 5$, the tactical costs are comparable and for $\gamma = 10$, the VC is almost double that of FCC. The Avg_{AT} values are always below 4 minutes and the Avg_{EC} is at most 87% of the drone battery. Under the centered setting, at most 45% of the drones consume more than 80% of the drone battery while this value increases to 63% if the marginal setting is selected.

Table 5: Computational results: larger instances

Instance	γ	FC configuration	FCC (%)	VC (%)	DC (%)	Avg_{AT} (min)	Avg_{EC} (kWh)	$> 80\%$	Obj	CPU (s)
In75-1	5	Centered	49.59	45.45	4.95	2.82	0.068	2	16.93	494.57
	10		32.97	60.44	6.58	2.82	0.071	2	12.73	388.12
In75-2	5	Centered	49.53	45.4	5.05	3.06	0.074	5	16.95	1533.54
	10		32.92	60.35	6.71	3.06	0.078	4	12.75	1138.42
In75-3	5	Centered	49.69	45.55	4.75	2.94	0.073	3	16.9	907.37
	10		33.06	60.61	6.32	2.94	0.071	3	12.7	273.07
In75-4	5	Centered	49.57	45.44	4.97	2.94	0.068	4	16.94	387.09
	10		32.95	60.42	6.61	2.94	0.074	3	12.74	170.71
In75-5	5	Centered	49.62	45.48	4.89	2.76	0.07	3	16.92	3538.15
	10		32.99	60.49	6.5	2.76	0.069	3	12.72	2171.62
In75-1	5	Marginal	49.36	45.25	5.37	3.30	0.083	5	17.01	717.78
	10		32.77	60.08	7.14	3.30	0.08	5	12.81	1344.51
In75-2	5	Marginal	49.38	45.26	5.35	3.30	0.087	6	17.01	887.89
	10		32.78	60.1	7.1	3.30	0.086	5	12.81	1044.79
In75-3	5	Marginal	49.41	45.29	5.28	3.54	0.083	6	16.99	1075.07
	10		32.81	60.16	7.01	3.54	0.08	5	12.79	524.17
In75-4	5	Marginal	49.38	45.27	5.34	3.48	0.081	5	17	1446.78
	10		32.78	60.11	7.09	3.48	0.082	7	12.8	957.2
In75-5	5	Marginal	49.39	45.27	5.32	3.42	0.08	2	17	801.57
	10		32.79	60.12	7.07	3.42	0.087	5	12.8	531.96

5 Conclusions

In this paper, we have investigated a drone delivery problem to address the tactical decisions arising in last-mile applications where the connection with operational plans is taken into account. The problem deals with the tactical selection of a subset of FCs to launch and retrieve the drones, and the fleet sizing decisions on the optimal number of drones to be employed. We have incorporated the non-linear and load-dependent energy consumption function into the definition of a load-indexed layered network, leading to the definition of a MILP that can be efficiently solved for instances with 50 and 75 customers. There are several fruitful directions for future research among

which the design of heuristic approaches to alleviate the computational burden and also the extension of the present model to account for en-route drone recharging.

References

[1] N. Agatz, P. Bouman, and M. Schmidt. Optimization approaches for the traveling salesman problem with drone. *Transportation Science*, 52 (4):965–981, 2018.

[2] J.-P. Aurambout, K. Gkoumas, and B. Ciuffo. Last mile delivery by drones: an estimation of viable market potential and access to citizens across european cities. *European Transport Research Review*, 11(1):1–21, 2019.

[3] M. E. Bruni and S. Khodaparasti. A variable neighborhood descent matheuristic for the drone routing problem with beehives sharing. *Sustainability (Switzerland)*, 14(16), 2022. doi: 10.3390/su14169978.

[4] C. Cheng, Y. Adulyasak, and L.-M. Rousseau. Drone routing with energy function: Formulation and exact algorithm. *Transportation Research Part B: Methodological*, 139:364–387, 2020.

[5] W.-C. Chiang, Y. Li, J. Shang, and T. L. Urban. Impact of drone delivery on sustainability and cost: Realizing the uav potential through vehicle routing optimization. *Applied energy*, 242:1164–1175, 2019.

[6] T.G. Crainic, G. Perboli, and N. Ricciardi. City Logistics. In T.G. Crainic, M. Gendreau, and B. Gendron, editors, *Network Design with Applications in Transportation and Logistics*, chapter 16, pages 507–537. Springer, Boston, 2021.

[7] V. Culpan. Wired. Watch how Swiss Post is delivering with drones. `https://www.wired.co.uk/article/swiss-delivery-drones`, 2015. Last access: 10/12/2022.

[8] DHL. DHL's parcelcopter: changing shipping forever. `https://www.dhl.com/discover/en-my/business/business-ethics/parcelcopter-drone-technology`, 2022. Last access: 10/12/2022.

[9] K. Dorling, J. Heinrichs, G. G. Messier, and S. Magierowski. Vehicle routing problems for drone delivery. *IEEE Transactions on Systems, Man, and Cybernetics: Systems*, 47(1):70–85, 2016.

[10] L. Du, X. Li, Y. Gan, and K. Leng. Optimal model and algorithm of medical materials delivery drone routing problem under major public health emergencies. *Sustainability*, 14(8):4651, 2022.

[11] L. Gouveia, M. Leitner, and M. Ruthmair. Layered graph approaches for combinatorial optimization problems. *Computers & Operations Research*, 102:22–38, 2019.

[12] S. Grogan, R. Pellerin, and M. Gamache. Using tornado-related weather data to route unmanned aerial vehicles to locate damage and victims. *OR Spectrum*, 43(4):905–939, 2021.

[13] M. Kanellos. Forbes. Google working on drones too. `https://www.forbes.com/sites/michaelkanellos/2014/08/29/google-working-on-drones-too/?sh=1d0c93ce79a7`, 2014. Last access: 10/12/2022.

[14] S. Kim, J. H. Kwak, B. Oh, D.-H. Lee, and D. Lee. An optimal routing algorithm for unmanned aerial vehicles. *Sensors*, 21(4):1219, 2021.

[15] S. J. Kim, G. J. Lim, J. Cho, and M. J. Côté. Drone-aided healthcare services for patients with chronic diseases in rural areas. *Journal of Intelligent & Robotic Systems*, 88(1):163–180, 2017.

[16] X. Li, P. Li, Y. Zhao, L. Zhang, and Y. Dong. A hybrid large neighborhood search algorithm for solving the multi depot uav swarm routing problem. *IEEE Access*, 9:104115–104126, 2021.

[17] Y. Liu, Z. Liu, J. Shi, G. Wu, and C. Chen. Optimization of base location and patrol routes for unmanned aerial vehicles in border intelligence, surveillance, and reconnaissance. *Journal of Advanced Transportation*, 2019, 2019.

[18] C. C. Murray and A. G. Chu. The flying sidekick traveling salesman problem: Optimization of drone-assisted parcel delivery. *Transportation Research Part C: Emerging Technologies*, 54:86–109, 2015.

[19] G. Perboli and M. Rosano. Parcel delivery in urban areas: Opportunities and threats for the mix of traditional and green business models. *Transportation Research Part C: Emerging Technologies*, 99:19–36, 2019. doi: 10.1016/j.trc.2019.01.006.

[20] G. Perboli, M. Rosano, M. Saint-Guillain, and P. Rizzo. A simulation-optimization framework for City Logistics. an application on multimodal last-mile delivery. *IET Intelligent Transport Systems*, 12(4):262–269, 2018.

[21] G. Perboli, L. Brotcorne, M. E. Bruni, and M. Rosano. A new model for Last-Mile Delivery and Satellite Depots management: The impact of the on-demand economy. *Transportation Research Part E: Logistics and Transportation Review*, 145:102–184, 2021.

[22] B. Rabta, C. Wankmüller, and G. Reiner. A drone fleet model for last-mile distribution in disaster relief operations. *International Journal of Disaster Risk Reduction*, 28:107–112, 2018.

[23] M. Torabbeigi, G. J. Lim, and S. J. Kim. Drone delivery scheduling optimization considering payload-induced battery consumption rates. *Journal of Intelligent & Robotic Systems*, 97(3):471–487, 2020.

[24] A. Troudi, S.-A. Addouche, S. Dellagi, and A. E. Mhamedi. Sizing of the drone delivery fleet considering energy autonomy. *Sustainability*, 10 (9):3344, 2018.

[25] E. Yakıcı. Solving location and routing problem for uavs. *Computers & Industrial Engineering*, 102:294–301, 2016.